



## NOTE

Pathology

# An atypical case of recurrent carotid body carcinoma in a young adult dog: Histopathological, immunohistochemical and electron microscopic study

Angeline Ping Ping TEH<sup>1)</sup>, Watanyoo PRATAKPIRIYA<sup>1)</sup>, Yuichi HIDAKA<sup>2)</sup>, Hiroyuki SATO<sup>3)</sup>, Takuya HIRAI<sup>1)</sup> and Ryoji YAMAGUCHI<sup>1)\*</sup>

<sup>1)</sup>Laboratory of Veterinary Pathology, Faculty of Agriculture, University of Miyazaki, Gakuen-kibanadai-nishi-1-1, Miyazaki 889-2192, Japan

<sup>2)</sup>Laboratory of Veterinary Surgery, Faculty of Agriculture, University of Miyazaki, Gakuen-kibanadai-nishi-1-1, Miyazaki 889-2192, Japan

<sup>3)</sup>Laboratory of Veterinary Radiology, Faculty of Agriculture, University of Miyazaki, Gakuen-kibanadai-nishi-1-1, Miyazaki 889-2192, Japan

**ABSTRACT.** A 3.5-year-old female Chihuahua was presented with complaint of neck pain, intermittent cough and dysphagia. Physical examination and diagnostic imaging of neck region revealed a solid and highly vascularized mass involving the retropharyngeal region. Histologically, the mass showed an atypical zellballen pattern which comprised of high density of type I chief cells with high nuclear cytoplasmic ratio and separated by delicate fibrovascular stroma. Immunoreactivity for neuroendocrine markers was diffusely positive in cytoplasm of tumor cells. Disseminated tumor emboli in external jugular vein were detected 6 months after initial surgery. An electron microscopic study revealed numerous electron-dense intracytoplasmic neurosecretory granules. Based on these findings, carotid body carcinoma was diagnosed.

**KEY WORDS:** carotid body carcinoma, dog, electron microscope, immunohistochemistry, zellballen pattern

*J. Vet. Med. Sci.*

79(4): 714–718, 2017

doi: 10.1292/jvms.16-0501

Received: 27 September 2016

Accepted: 15 February 2017

Published online in J-STAGE:

27 February 2017

Carotid body tumor, a neuroendocrine tumor of the chemoreceptor organ-carotid body, which is located at the bifurcation of the common carotid artery in the cranial cervical area and served as a sensitive barometer for regulation of respiration and circulation; has been infrequently reported in dogs [4, 5, 14, 16]. These rare neuroendocrine tumors with strong vascularization have been reported less than 80 canine cases till 1992 since they were first described in dogs in 1957 [13], and in recent 25 years, about 8 cases of carotid body tumors were reported where 7 of them were malignant [2, 5, 9, 14, 16]. Chemoreceptor tumors, also known as chemodectomas or non-chromaffin paragangliomas, develop principally in the aortic and carotid bodies, with instances of aortic body tumors (ABTs) being 5 to 10 times more frequent [5, 7]. Brachycephalic breeds of dogs, such as Boxers and Boston terriers, are predisposed to these tumors [4, 12, 13]. Thirty percent of reported cases of carotid body tumors in dogs revealed metastases evidence and thus tend to be more malignant than ABTs which are 22% [13, 14]. Previous studies have reported that median age for dogs with carotid body tumors was 10 years with a range of 8–15 years [7, 13]. To the best of our knowledge, this paper is the first report of the recurrence of a carotid body carcinoma in a young adult Chihuahua dog, and was not histologically consistent with previously-reported findings indicating malignancy, mitotic figures and cellular pleomorphism.

Chemoreceptor organs comprise of two major types of cells: neuroendocrine cells (type I) and supporting or sustentacular cells (type II) [1]. The type I cells, which are derived from the neural crest, are considered as chief cells, and they contain numerous secretory granules, such as catecholamine and serotonin. The type II sustentacular cells are satellite elements which lack of neurosecretory granules [1]. Zellballen pattern is defined as nest-like clusters of uniform, round-to-polygonal type I cells surrounded by delicate richly vascular tissue and type II cells, which is a pattern characteristic of chemodectoma or paraganglioma [11]. In benign chemodectoma, the type I cells usually show low nuclear to cytoplasmic (N:C) ratio. The malignant variant of carotid body tumor, with metastases reported in the brain, lung, heart, bronchial and mediastinal lymph nodes, liver, pancreas, kidney and bone, is recorded in about 21 cases in past 42 years [2, 4, 7, 9, 13, 14, 16]. To date, there are very little details about histopathological, immunohistochemical and electron microscope findings of carotid body carcinoma in dogs. In this paper, we

\*Correspondence to: Yamaguchi, R., Laboratory of Veterinary Pathology, Faculty of Agriculture, University of Miyazaki, Gakuen-kibanadai-nishi-1-1, Miyazaki 889-2192, Japan. e-mail: aod40zu@cc.miyazaki-u.ac.jp

©2017 The Japanese Society of Veterinary Science



This is an open-access article distributed under the terms of the Creative Commons Attribution Non-Commercial No Derivatives (by-nc-nd) License. (CC-BY-NC-ND 4.0: <https://creativecommons.org/licenses/by-nc-nd/4.0/>)

describe a first atypical case of carotid body carcinoma, with histological characteristic, immunohistochemical malignancies evaluation and electron microscopic findings.

A 3.5-year-old spayed female Chihuahua was presented for evaluation of a history of neck pain, intermittent cough and dysphagia. On physical examination, a left lateral neck mass with poor mobility was found caudal to the mandible. Auscultation of left heart apex revealed a 3/6 systolic heart murmur. Results of complete blood count were within normal limits, and biochemistry test results revealed mildly elevated levels of liver enzymes [aspartate aminotransferase: 23  $\mu$ /l, reference interval: 13–15  $\mu$ /l; and alkaline phosphatase (AP): 233  $\mu$ /l, reference interval: 1–114  $\mu$ /l] and glucose (124 mg/dl, reference interval: 79–119 mg/dl). Radiographs exhibited an abnormal mass in lateral neck region with no evidence of lung metastasis. Ultrasonography examination revealed a highly vascularized mass of the size of 27.0  $\times$  37.5 mm in the left lateral neck. A transverse computed tomography (CT) image of the third cervical vertebra revealed a mass adjacent to left side of the larynx, laterally displacing left common carotid artery and left jugular vein (Fig. 1).

The mass, which engulfed various neck structures, along with ligation of vagus nerve, internal jugular vein, common carotid artery and external carotid artery was surgically removed and sent for histopathological diagnosis. The macroscopic aspect showed a firm, fibrous, encapsulated mass with heavy vascularization. The cut surface revealed a greyish-white solid mass with a coarsely multi-lobulated structure (Supplementary Fig. 1). Cytology revealed clusters of round-to-oval tumor cells with high nuclear to cytoplasmic ratio (N:C) and moderate anisokaryosis (Supplementary Fig. 2).

Histologically, the mass was encapsulated by fibrous tissue. Type I tumor cells were separated by delicate type II sustentacular cells and arranged in a solid nested pattern (Fig. 2). Pyknotic nuclei were commonly found among the high density of type I tumor cells (Fig. 2). Predominant type I cell had indistinct cell borders with uniform, spherical-to-oval, centrally located basophilic nucleus and scanty cytoplasm. Nuclear density was high with salt and pepper chromatin. Mitotic figures were rarely observed in the tumor sections. No colloidal secretion was noticed. Tumor cells infiltrated into the fibrous capsule and adjacent connective tissue. Necrosis and hemorrhage were observed throughout the tumor. Tumor was well vascularized, and tumor emboli were found among the blood vessels. The external carotid artery was surrounded by the tumor mass.

Immunohistochemical analysis was performed using several primary antibodies manufactured from Dako, Glostrup, Denmark. Cytokeratin (CK) AE1/3, thyroglobulin (TGB), thyroid transcription factor-1 (TTF-1), calcitonin, chromogranin A (CrA), neuron-specific enolase (NSE), synaptophysin, S-100, neurofilament protein, Ki-67 and von Willebrand factor (vWF) were incubated on sections of 4  $\mu$ m paraffin embedded masses, respectively. Tumor cells showed strong positive cytoplasmic staining with 3, 3'-diaminobenzidine solution (DAB; Sigma-Aldrich, St. Louis, MO, U.S.A.) in a horseradish peroxidase (HRP) system for CrA, NSE and synaptophysin (Fig. 3), while they were negative for CK AE1/3, TGB, TTF-1, calcitonin, S-100, neurofilament protein and Ki-67. Unilateral carotid body carcinoma was diagnosed. Synaptophysin-positive tumor emboli were observed in the lumen of the blood vessels. Subsequently, double immunohistochemistry staining for vWF, visualized using DAB in a HRP system, and CrA, visualized using Fast red II, in an alkaline phosphatase system revealed evidence of invasion of tumor cells through the basement membrane of the blood vessel (Fig. 4).

Recurrent carotid body carcinoma with dissemination into the external jugular vein occurred six months after initial surgical resection. Histopathological findings revealed the same histopathological findings as previously described in which tumor cells comprised of high density of type I cells and arranged in atypical zellballen pattern with numerous pyknotic nuclei (Fig. 5). Cross section of external jugular vein revealed that disseminated tumor emboli occluded almost entire lumen of the blood vessel (Supplementary Fig. 3). In addition, the results of immunohistochemical examination of tumor emboli were the same as previous biopsy. The dog was euthanized one month later due to metastasis to dorsal cerebellum and pons confirmed by magnetic resonance imaging (MRI) scan (Fig. 6) and poor prognosis. Unfortunately, autopsy was not permitted.

Ultrastructural examinations of carotid body carcinoma were done by transmission electron microscopy (TEM) using deparaffinized paraffin-embedded blocks. Five  $\mu$ m thick selected paraffin section was cut and mounted on glass slides. Reprocessing was done by deparaffinization followed by rehydration. The sample was re-fixed in 2% paraformaldehyde and 2.5% glutaraldehyde in 0.1 M cacodylate buffer (pH 7.4) for 2 hr at 4°C and followed by washing with 0.1 M cacodylate buffer (pH 7.4) at 4°C for 5 min 2 times. Post-fixation was done with 1% osmium tetroxide in 0.1 M cacodylate buffer (pH 7.4) for 2 hr at 4°C, followed by washing with 0.1 M cacodylate buffer (pH 7.4) at 4°C for 10 min. The specimen was dehydrated through a series of ethanols and propylene oxide. The specimen was embedded in Epon for 24 hr at 60°C followed by staining with 0.1% toluidine blue. Then, specimen was cut into ultrathin section and stained with 0.5% uranyl acetate and 3% lead citrate at 20°C, for 30 min and 7 min, respectively at 20°C. The section was observed with transmission electron microscopy HT7700 (Hitachi, Tokyo, Japan). Tumor cells included numerous dense granules with size approximately 100 nm in diameter and cytoplasmic glycogen pools (Fig. 7). Nuclei were generally round or oval with dispersed chromatin. Other organelles were difficult to recognize due to deterioration of the cell structure.

With the definitive diagnosis of carotid body carcinoma, the clinical manifestations can be explained coherently. The tumor had invaded the vagus nerve, which led to the neck pain. Dysphagia was caused by compression of the space occupying tumor on the esophagus. The systolic murmur was initiated by pulsatile protuberance, because these tumors are highly vascular in nature and they have a marked chemoreceptor function mimicking the normal carotid body. The tumor clinically appeared as a slow-growing mass located near the angle of the mandibula that usually had a free lateral movement but limited cranio-caudal mobility [4].

Neck masses always exhibit a diagnostic challenge, because of its compact anatomical structure, involving several adjacent organs, such as blood vessels, nerves, parathyroid, thyroid, muscles, esophagus and trachea. Imaging modalities, including radiography, ultrasonography, CT scan and magnetic resonance imaging are usually required for diagnosis. On the basis of



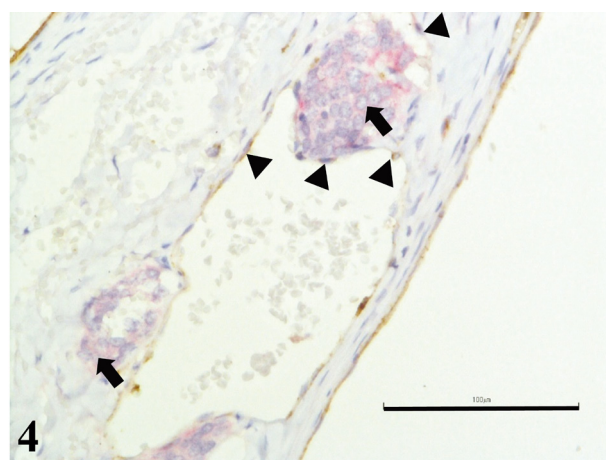
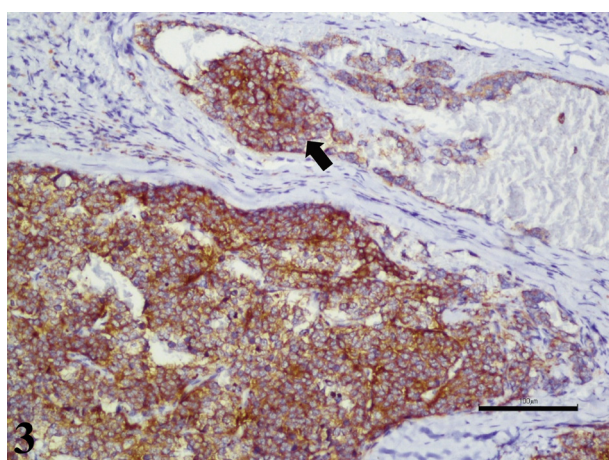
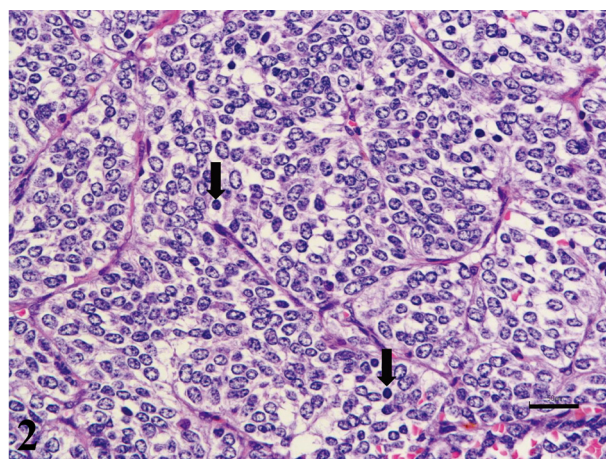
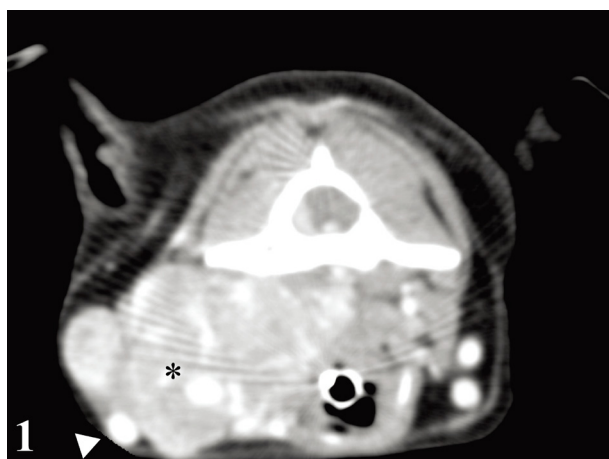


**Fig. 1.** Carotid body carcinoma; dog. Transverse computed tomography image at the third cervical vertebra revealed mass (asterisk) adjacent to the left side of larynx, displacing left common carotid artery and left jugular vein laterally (arrowhead).

**Fig. 2.** Carotid body carcinoma; dog. The atypical zellballen pattern showing high density of type I tumor chief cells with high N:C ratio, and indistinct cell borders are divided into lobules by differing amounts of fibrovascular stroma. Pyknotic nuclei were commonly found among the high density of tumor cells (arrows). Hematoxylin and eosin (HE). Bar=50  $\mu$ m.

**Fig. 3.** Carotid body carcinoma; dog. Expression of synaptophysin showing many granules in cytoplasm of tumor cells. Adjacent blood vessel revealed intravascular synaptophysin-positive tumor cells infiltration (arrow). Immunohistochemistry for synaptophysin. Bar=100  $\mu$ m.

**Fig. 4.** Carotid body carcinoma; dog. Double immunohistochemistry staining for von Willebrand Factor VIII, visualized using DAB in a HRP system (brown stain) (arrowheads), and CrA, visualized using Fast red II, in an alkaline phosphatase system (red stain) revealed evidence of invasion of tumor cells (arrows) through the basement membrane of the blood vessel. Bar=100  $\mu$ m.

histopathology alone, it is difficult to differentiate carotid body tumor from parathyroid carcinoma and solid thyroid carcinoma, because all of them exhibit hyper-cellularity, hyper-vascularity and homogeneity, and they are mostly composed of chief cells that are arranged in trabecular patterns with collagen fibrous bands [3]. Thus, immunohistochemistry is crucial in the diagnosis of carotid body tumor, where the cytoplasm of the tumor contains neurosecretory and dense core granules that immunohistologically express neuroendocrine markers, such as NSE, synaptophysin and CrA [2, 15, 17], and negative staining in cytokeratin sufficiently ruled out thyroid and parathyroid tumors. Neuroendocrine tumors can be grouped into subtypes of epithelial origin and neural origin based on the CK or neurofilament expression, respectively [6]. Neural origin neuroendocrine tumors like paraganglioma usually have negative staining of CK AE1/3.

To date, there are no histopathological or immunohistochemical clear-cut criteria to predict the malignancy behavior of carotid body tumors, because benign tumor often appears malignant and malignant tumor may appear benign [4]. Histologically, a normal carotid body structure, which has nest-like clusters of uniform and round-to-polygonal chief cells that are surrounded by delicate rich vascular tissue and sustentacular cells, resembles the zellballen structure of carotid body tumor, making the determination of malignancy more difficult [5]. A previous study of carotid body tumors was graded histologically to the following 3 criteria: mitotic figures, cellular pleomorphism, and invasion into vessel [13]. The pathological characteristics of this current case are low-cellular pleomorphism with a low-mitotic figure (appeared benign), and with atypical zellballen pattern which comprised of high density of

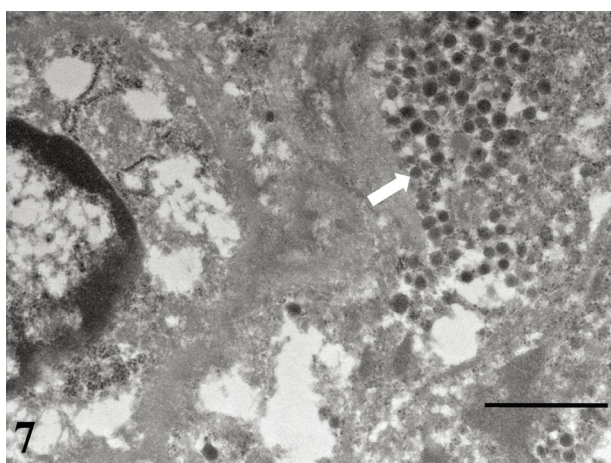
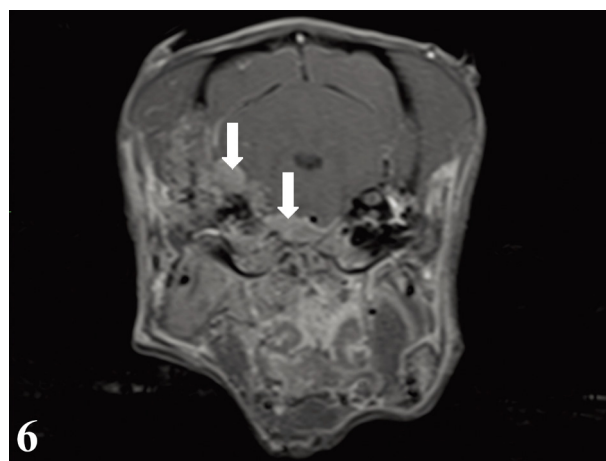
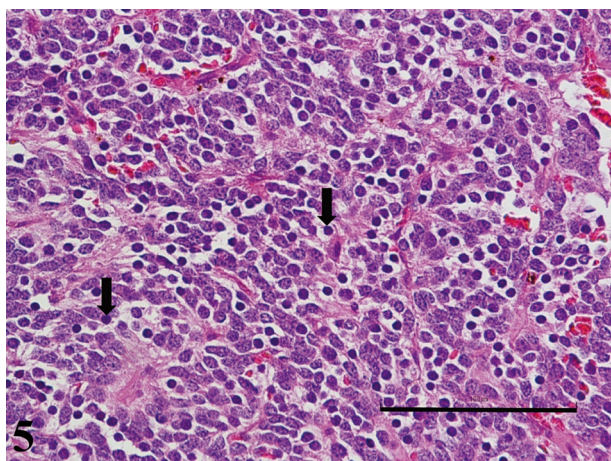


**Fig. 5.** Carotid body carcinoma; dog. Six months after initial surgical resection, recurrent carotid body carcinoma disseminated into the external jugular vein. Histopathological findings revealed atypical Zellballen pattern with high type I cell density and numerous pyknotic nuclei (arrows). HE. Bar=100  $\mu$ m.

**Fig. 6.** Carotid body carcinoma; dog. Brain metastasis. Transverse images of magnetic resonance imaging at caudal brain area revealed a hyper-intense mass (arrows) involving left ventral cerebellum and left dorsal pons.

**Fig. 7.** Carotid body carcinoma; dog. Electron microscopic study of carotid body carcinoma revealed electron dense neurosecretory type granules (arrow). TEM. Bar=1  $\mu$ m.

type I tumor cells and N:C ratio with frequent pyknotic nuclei, and vascular invasion (appeared malignant). Many previous reports have indicated that the prevalence of mitotic figures in chemodectomas is low and does not correlate well with malignant behavior [2, 4, 10, 17]. In a study of malignant potential of canine ABTs, it seems difficult to grade ABTs on the basis of mitotic activity and the presence or absence of vascular invasion, because no distant metastases occurred even though their study object showed tumor cells within the adjacent blood vessels and lymphatics lumen [17]. Therefore, mitotic figures, cellular pleomorphism and vascular invasion in carotid body tumors may not be reliable for malignancies diagnosis, and presence of metastasis is the only definite criterion for diagnosis of a malignant carotid body tumor. In this case, there is vascular invasion and evidence of metastasis to the brain. Thus, vascular invasion should be always assumed an indication of malignancy and warranted a close clinical surveillance.

Regarding immunohistochemistry, analyses of canine ABTs have been performed to identify the expression of NSE, synaptophysin, CrA and S-100 and establish the criteria for tumor grading [1, 2, 12]. These studies have demonstrated that the expression of CrA decreased with increasing malignancy owing to degranulation of type I cells, indicating low synthesis of granules. Contradicting to a reported study, the current case of malignant tumor showed strong CrA staining and contained electron-dense neurosecretory granules, indicating high presence of granules. S-100 was positive only in sustentacular cells and was negative in tumor cells. S-100 is considered the most useful marker for the evaluation of tumor grades by a previous study that showed the labeling intensity of sustentacular cells was inversely related to the tumor grade [1, 8]. The density of sustentacular cells was gradually lost in tumors with increasing degrees of malignancy in ABTs [1]. As demonstrated in this case, the negative staining for S-100 suggested its malignant potential. A small number of Ki-67 positive cells coincide with low mitotic activity in these tumors. However, because there was no correlation between mitotic activities and the tendency for metastases, there is little value for tumor grading [2, 4, 10, 17]. The immunoreactive intensity of NSE and synaptophysin has been reported to be similar in benign and malignant tumor cells [2, 12].

The results of the present study showed that the tumor was strongly immunopositive for CrA, synaptophysin and NSE, and the lack of S-100 immunoreaction, combined with the evidence of dissemination tumor emboli, suggested a considerably malignant outcome. Histological findings of Zellballen structure; such as high type I cellular density with high N:C ratio and numerous pyknotic nucleus in this case; are highly suggestive for a malignancy diagnosis in chemodectoma. Further investigations of the structure of Zellballen pattern should be conducted to aid with the prognosis in future encounter of similar cases. In conclusion, this case has provided the evidences of malignancy and presented a high type I cell density of Zellballen pattern which has not been discussed in previous studies of carotid body carcinoma.



## REFERENCES

1. Aresu, L., Tursi, M., Iussich, S., Guarda, F. and Valenza, F. 2006. Use of s-100 and chromogranin a antibodies as immunohistochemical markers on detection of malignancy in aortic body tumors in dog. *J. Vet. Med. Sci.* **68**: 1229–1233. [[Medline](#)] [[CrossRef](#)]
2. Brown, P. J., Rema, A. and Gartner, F. 2003. Immunohistochemical characteristics of canine aortic and carotid body tumours. *J. Vet. Med. A Physiol. Pathol. Clin. Med.* **50**: 140–144. [[Medline](#)] [[CrossRef](#)]
3. Cheville, N. F. 1972. Ultrastructure of canine carotid body and aortic body tumors. Comparison with tissues of thyroid and parathyroid origin. *Vet. Pathol.* **9**: 166–189. [[Medline](#)] [[CrossRef](#)]
4. Dean, M. J. and Straffuss, A. C. 1975. Carotid body tumors in the dog: a review and report of four cases. *J. Am. Vet. Med. Assoc.* **166**: 1003–1006. [[Medline](#)]
5. Deim, Z., Szalay, F., Glávits, R., Bauer, A. and Cserni, G. 2007. Carotid body tumor in dog: a case report. *Can. Vet. J.* **48**: 865–867. [[Medline](#)]
6. DeLellis, R. A. 2001. The neuroendocrine system and its tumors: an overview. *Am. J. Clin. Pathol.* **115** Suppl: S5–S16. [[Medline](#)]
7. Hayes, H. M. and Sass, B. 1988. Chemoreceptor neoplasia: a study of the epidemiological features of 357 canine cases. *Zentralbl. Veterinarmed. A* **35**: 401–408. [[Medline](#)] [[CrossRef](#)]
8. Kliwer, K. E., Wen, D. R., Cancilla, P. A. and Cochran, A. J. 1989. Paragangliomas: assessment of prognosis by histologic, immunohistochemical, and ultrastructural techniques. *Hum. Pathol.* **20**: 29–39. [[Medline](#)] [[CrossRef](#)]
9. Kromhout, K., Gielen, I., De Cock, H. E., Van Dyck, K. and van Bree, H. 2012. Magnetic resonance and computed tomography imaging of a carotid body tumor in a dog. *Acta Vet. Scand.* **54**: 24. [[Medline](#)] [[CrossRef](#)]
10. Kurtz, H. J. and Finco, D. R. 1969. Carotid body and aortic body tumors in a dog--a case report. *Am. J. Vet. Res.* **30**: 1247–1251. [[Medline](#)]
11. Luna, M. A. and Pineda-Daboin, K. 2006. Paraganglioma. p. 274. In: *Pathology of the Head and Neck*, 2nd ed. (Cardesa, A., Sloodweg, P. J., Gale, N. and Franchi, A. eds.), Springer-Verlag, Berlin.
12. Noszczyk-Nowak, A., Nowak, M., Paslawska, U., Atamaniuk, W. and Nicpon, J. 2010. Cases with manifestation of chemodectoma diagnosed in dogs in Department of Internal Diseases with Horses, Dogs and Cats Clinic, Veterinary Medicine Faculty, University of Environmental and Life Sciences, Wrocław, Poland. *Acta Vet. Scand.* **52**: 35. [[Medline](#)] [[CrossRef](#)]
13. Obradovich, J. E., Withrow, S. J., Powers, B. E. and Walshaw, R. 1992. Carotid body tumors in the dog. Eleven cases (1978–1988). *J. Vet. Intern. Med.* **6**: 96–101. [[Medline](#)] [[CrossRef](#)]
14. Okajima, M., Shimada, A., Morita, T., Yoshikawa, M. and Nishida, K. 2007. Multiple osseous metastases of a carotid body tumor in a dog. *J. Vet. Med. Sci.* **69**: 297–299. [[Medline](#)] [[CrossRef](#)]
15. Pávai, Z., Orosz, Z., Horváth, E., Seres-Sturm, L. and Jung, J. 2001. Immunohistochemical features of paragangliomas. *J. Cell. Mol. Med.* **5**: 311–316. [[Medline](#)] [[CrossRef](#)]
16. Romanucci, M., Malatesta, D., Berardi, I., Pugliese, G., Fusco, D. and Della Salda, L. 2014. Cytological, histological and ultrastructural nuclear features of monster cells in a canine carotid body carcinoma. *J. Comp. Pathol.* **151**: 57–62. [[Medline](#)] [[CrossRef](#)]
17. Yamamoto, S., Fukushima, R., Hirakawa, A., Abe, M., Kobayashi, M. and Machida, N. 2013. Histopathological and immunohistochemical evaluation of malignant potential in canine aortic body tumours. *J. Comp. Pathol.* **149**: 182–191. [[Medline](#)] [[CrossRef](#)]